Cerebral metabolic and cognitive decline in persons at genetic risk for Alzheimer's disease

Gary W. Small*†‡, Linda M. Ercoli†, Daniel H. S. Silverman§, S.-C. Huang§, Scott Komo†, Susan Y. Bookheimer†¶, Helen Lavretsky†, Karen Miller†, Prabha Siddarth†, Natalie L. Rasgon†, John C. Mazziotta§¶‖, Sanjaya Saxena†, H. M. Wu§, Michael S. Mega‖, Jeffrey L. Cummings†‖, Ann M. Saunders**, Margaret A. Pericak-Vance**, Allen D. Roses**††, Jorge R. Barrio§, and Michael E. Phelps§

*Center on Aging and †Department of Psychiatry and Biobehavioral Sciences, Neuropsychiatric Institute, 760 Westwood Plaza, Los Angeles, CA 90024; Departments of §Molecular and Medical Pharmacology and ‖Neurology, and ¶Brain Mapping Center, University of California, Los Angeles, CA 90095; **Department of Medicine, Duke University Medical Center, Durham, NC 27710; and ††Glaxo Wellcome Research and Development, Research Triangle Park, NC 27709

Contributed by Michael E. Phelps, March 10, 2000

The major known genetic risk for Alzheimer's disease (AD), apolipoprotein E-4 (APOE-4), is associated with lowered parietal, temporal, and posterior cingulate cerebral glucose metabolism in patients with a clinical diagnosis of AD. To determine cognitive and metabolic decline patterns according to genetic risk, we investigated cerebral metabolic rates by using positron emission tomography in middle-aged and older nondemented persons with normal memory performance. A single copy of the APOE-4 allele was associated with lowered inferior parietal, lateral temporal, and posterior cingulate metabolism, which predicted cognitive decline after 2 years of longitudinal follow-up. For the 20 nondemented subjects followed longitudinally, memory performance scores did not decline significantly, but cortical metabolic rates did. In APOE-4 carriers, a 4% left posterior cingulate metabolic decline was observed, and inferior parietal and lateral temporal regions demonstrated the greatest magnitude (5%) of metabolic decline after 2 years. These results indicate that the combination of cerebral metabolic rates and genetic risk factors provides a means for preclinical AD detection that will assist in response monitoring during experimental treatments.

apolipoprotein E | positron emission tomography | cerebral glucose metabolism | age-associated memory impairment

Alzheimer's disease (AD) accounts for approximately two-thirds of late-life dementias, afflicting an estimated 8% of people age 65 years and older (1). In the United States alone, AD victims total nearly four million, and annual cost estimates, including caregiver productivity losses and costs of medical, long-term, and home care, approach $90 billion (2, 3). The disease's gradual decline in memory, other cognitive functions, behaviors, and daily functions progress until patients eventually require total care from others (4).

Mild memory complaints build gradually years before patients develop dementia, and neurofibrillary tangles (5) and neuritic plaques (6), the neuropathological hallmarks of AD, are present in older persons with memory complaints too mild to warrant a diagnosis of dementia. Amyloid deposits have been observed in middle-aged nondemented persons decades before they reach the age at risk for late-onset AD (7). Moreover, diffuse plaques in nondemented elderly persons are associated with an accelerated age-related cortical cholinergic deficit, which could represent a clinical stage preceding dementia (8). Such observations have stimulated interest in "preclinical" AD markers aimed at identifying candidates who may benefit from novel antidementia treatments. Randomized, placebo-controlled trials of cholinesterase inhibitors, anti-oxidants, and anti-inflammatory agents are already in progress for such conditions as mild cognitive impairment (9) or age-associated memory impairment (AAMI) (10). These experimental drug trials use standard clinical examination methods to identify subjects and follow cognitive decline (4, 11). Because many people with mild memory complaints do not progress to AD, more sensitive and specific tools that predict future cognitive decline would heighten accuracy in detecting preclinical AD and facilitate more effective early intervention.

Combining genetic risk and functional brain imaging measures is a promising preclinical AD detection strategy (12). Genetic studies have identified an association between the apolipoprotein E-4 (APOE-4) allele on chromosome 19 and the common form of AD that begins after age 60 (13). The APOE-4 allele has a dose-related effect on increasing risk and lowering onset age for late-onset familial and sporadic AD (14), whereas APOE-2 appears to confer protection (15). The APOE-4 allele may have a modest effect in predicting cognitive decline in older persons, but APOE genotype alone is not considered a useful predictor in nondemented persons (16).

Positron emission tomography (PET) (17, 18) with [^{18}F]fluorodeoxyglucose (FDG) allows the noninvasive determination of local cerebral glucose metabolic rate in humans through the use of a tracer kinetic model (19, 20). PET determinations of glucose metabolism in AD show a consistent pattern of reduced cerebral glucose utilization beginning in parietal and temporal regions and later spreading to prefrontal cortices. Such patterns have been observed in subjects with questionable dementia (12) several years before they develop clinically confirmed probable AD, and they can differentiate AD from the metabolic abnormalities of other dementias, including Lewy body dementia, vascular dementia, and frontotemporal dementia (21). PET offers a marker that is sensitive to mild, early brain changes, and gradual progression; therefore, it is ideal for monitoring experimental therapeutic treatments early in the disease before substantial neuronal death occurs.

Our initial observation of parietal hypometabolism in nondemented people with a single copy of APOE-4 and a familial risk for AD (12) has been replicated in APOE homozygotes (4/4 genotype) and extended to other brain regions, including posterior cingulate, and dorsolateral prefrontal and temporal cortices (22). In the present study, we determine the consistency of such findings in a separate and larger subject cohort and show that they predict future cognitive and metabolic decline.

Abbreviations: AD, Alzheimer's disease; APOE, apolipoprotein E; PET, positron emission tomography; ROI, region of interest; AAMI, age-associated memory impairment; FDG, [^{18}F]fluorodeoxyglucose; SPM, statistical parametric mapping.

See commentary at www.pnas.org/cgi/doi/10.1073/pnas.120178897

‡To whom correspondence should be addressed. e-mail: gsmall@mednet.ucla.edu.

The publication costs of this article were defrayed in part by page charge payment. This article must therefore be hereby marked "*advertisement*" in accordance with 18 U.S.C. §1734 solely to indicate this fact.

Article published online before print: *Proc. Natl. Acad. Sci. USA*, 10.1073/pnas.090106797. Article and publication date are at www.pnas.org/cgi/doi/10.1073/pnas.090106797

Methods

Subjects (61 Caucasians, 3 Asians, 1 Hispanic) were right-handed, in the 50- to 84-year-old age range (mean ± SD = 67.3 ± 9.4 years), and recruited through newspaper advertisements for people with memory complaints and/or dementia family histories, media coverage, and other referrals. Subjects were included with or without a family history of AD (defined as ≥1 first-degree relative with a clinical diagnosis of AD). All subjects received neurologic, psychiatric, and neuropsychological evaluations and routine screening laboratory tests to rule out treatable causes of cognitive impairment and to detail cognitive performance (4, 23–26). Subjects with any other neurological, medical, or psychiatric condition (e.g., depression) that could affect memory or cognitive processing were excluded. None of the subjects participated in our previous study of APOE and PET (12). Of the 65 subjects, 54 were nondemented and 11 were demented and diagnosed with probable AD (27).

The 54 nondemented subjects were aware of a gradual onset of mild memory complaints (e.g., misplacing familiar objects, difficulty remembering names). Of the 573 persons who volunteered to participate because of minor memory concerns, 508 were excluded for a variety of reasons (e.g., medication use, concurrent medical or psychiatric illness). All 54 nondemented subjects assessed at baseline receive follow-up evaluations at 2-year intervals. The 20 subjects in the present longitudinal study are a subset of the 54 nondemented subjects who have already returned for follow-up memory performance and PET scan studies 2 years after baseline assessment (mean ± SD for follow-up was 27.9 ± 1.7 months).

DNA was obtained from blood samples to determine APOE genotypes by using standard techniques, as described (13). The 54 nondemented subjects included 27 APOE-4 carriers and 27 subjects without APOE-4. The subset of 20 nondemented subjects available for follow-up included 10 APOE-4 carriers and 10 subjects without APOE-4. The 11 AD subjects (27) were included as a baseline comparison group without regard to APOE status, because previous studies have found that cerebral metabolic patterns do not vary according to APOE genotype in AD patients (28, 29).

Subjects underwent PET imaging as described (19, 20). In brief, the subjects were scanned in the supine position with low ambient noise, and their eyes and ears were not occluded. Intravenous lines were placed 10–15 min before tracer injection of 370 MBq of FDG. Scans were performed 40 min after FDG injection by using the CTI/Seimens 831–08 or the CTI 962 scanner (Seimens, Hoffman Estates, IL). Because two scanners were used to acquire images (because of scanner availability), tomographic images were reconstructed and axially smoothed to give the same spatial resolutions (full width at half maximum was 0.65 cm in the axial plane and 0.8 cm in the image plane). Scans were acquired parallel to the canthomeatal line; a transmission measurement was used for attenuation correction.

Baseline MRI brain scans were obtained by using either a 1.5 Tesla magnet (General Electric-Signa, Milwaukee, WI) or a 3 Tesla magnet (General Electric Signa). At follow-up, all subjects were scanned by using the 3 Tesla magnet. Thirty-six transaxial planes were collected throughout the brain volume, superior to the cerebellum. A double echo, fast spin echo series using a 24-cm field of view and 256 × 256 matrix with 3 mm/0 gap (TR = 6000 [3T] and 2000 [1.5T]; TE = 17/85 [3T] and 30/90 [1.5T]) was acquired for MRI registration with PET for improving anatomical localization of metabolism within individual structures of the brain. An intermodality image coregistration program (30) that uses image segmentation and simulation as preprocessing procedures was used to coregister PET and baseline MRI images of each subject. Both region of interest (ROI) and statistical parametric mapping (SPM) analyses then were performed.

Rules for ROI drawing were based on the identification of gyral and sulcal landmarks with respect to the atlas of Talairach and Tournoux (31). Regions involving memory processing and AD were determined manually on registered MRI scans for right and left hemispheres for inferior parietal (cortex surrounding the intraparietal sulcus, including the supramarginal gyrus and angular gyrus); posterior cingulate (ascending portion of the posterior cingulate gyrus, retrosplenial region, just posterior to the corpus callosum); dorsolateral prefrontal (middle frontal gyrus including the gray matter surrounding the inferior frontal sulcus, corresponding roughly to Brodmann's areas 9 and 46); medial temporal (hippocampus and amygdala, just lateral to the pons), and inferior temporal (cortex surrounding the inferior temporal sulcus at the base of the temporal lobes) cortices; and whole brain (including cortex, subcortical gray matter, and midbrain to the level of the pons, and excluding cerebellum).

Two persons drew the ROIs, and interrater reliability, measured by calculating the spatial overlap of ROIs drawn twice, was assessed in 10 subjects to ensure reliability ≥0.85 (mean ± SD = 0.93 ± 0.04). ROI values were normalized to the whole brain value, and only the top 30% pixel values within each ROI were used as a compromise between the needs to minimize both the image statistical noise and the variability of ROI drawing on the calculated ROI values (32). Statistical tests involving the two nondemented groups included only those ROIs significantly different among the three subject groups after correcting for multiple comparisons.

For comparisons between the two nondemented groups at baseline and follow-up, PET data also were subjected to SPM analysis (33, 34) by using the SPM96 software package (Wellcome Department of Cognitive Neurology, Functional Imaging Laboratory, London). Briefly, images were coregistered and reoriented into a standardized coordinate system (33), spatially smoothed, and normalized to mean global activity, as described (35), with the exception that a three-dimensional Gaussian smoothing filter that was applied to images before statistical analysis had a full-width half-maximum of 16 mm. The pooled data then were assessed with the *t*-statistic on a voxel-by-voxel basis to identify the profile of voxels that significantly differed between genotypic groups, or (in the case of the longitudinally followed sample) differed within a genetic risk group at two points in time. The probability of finding by chance any region containing its voxel of maximal significance was adjusted for multiple comparisons by a Bonferroni-type correction, and the region as a whole was considered significant only if that adjusted probability was <0.05 (36).

Written informed consent was obtained in accordance with the procedures set by the University of California, Los Angeles, Human Subjects Protection Committee. All clinical assessments were performed within 3 weeks of PET scanning. Genetic test results were not released to participants. Clinical diagnoses were made with investigators blind to genetic data; image data were analyzed and ROIs determined with investigators blind to clinical and genetic findings.

Results

Subject groups were similar in mean age at examination, dementia onset age within families, educational achievement level, frequency of women, or family history of AD (Table 1). Genotypes of the demented group included one with 4/4, five with 3/4, and five with 3/3, indicating a proportion of APOE-4 subjects (55%) similar to that of other dementia groups reported in the literature (13, 16). The nondemented APOE-4 carriers were all heterozygotes (3/4 genotype) except for two subjects who were homozygotes (4/4). Of the nondemented subjects without APOE-4, 25 had the 3/3 genotype and two had the 2/3

Table 1. Baseline demographic and clinical characteristics of subject groups

Characteristic	Dementia group ($n = 11$)	Nondemented groups: With APOE-4 ($n = 27$)	Nondemented groups: Without APOE-4 ($n = 27$)
Age (yr)	72.2 ± 11.3	65.9 ± 8.8	66.8 ± 8.9
Women	6 (55)	16 (59)	13 (48)
Family history of AD*	6 (55)	18 (67)	13 (48)
Mean onset age†	69.0 ± 8.6	70.3 ± 6.2	68.8 ± 6.1
Education (yr)	14.5 ± 2.5	15.5 ± 2.6	16.0 ± 2.7
Mini-mental state exam‡	18.6 ± 3.7	28.4 ± 1.6	29.2 ± 1.2
Delayed paragraph recall§	0.3 ± 0.8	18.7 ± 8.5	21.8 ± 6.7
Buschke-Fuld total recall¶	34.6 ± 20.3	94.7 ± 18.2	101.6 ± 18.8
Benton visual errors‖	16.4 ± 5.0	4.3 ± 2.4	4.7 ± 2.8

Values are reported as mean ± SD or number (percent).

*Calculated only from subgroup with a family history (>1 first-degree relative with clinical or autopsy-confirmed AD).

†Onset age of demented patients or demented family members.

‡$F = 124.62$, df = 2, $P < 0.0001$; median score = 28 (65–69 years) (23).

§$F = 24.8$, df = 2,54, $P < 0.0001$; norms = 16.8 ± 8.1 (65–69 years) (24).

¶$F = 49.1$, df = 2,61, $P < 0.0001$; norms = men: 81.4 ± 17.4, women: 95.9 ± 19.1 (25).

‖$F = 64.8$, df = 2,62, $P < 0.0001$; norms = 5 ± 5 (65–74 years) (26).

genotype. The 27 nondemented APOE-4 carriers included 21 (78%) who met criteria for AAMI, 3 (11%) who met criteria for mild cognitive impairment, and 3 (11%) who met neither criteria. The 27 nondemented subjects without APOE-4 included 23 (85%) who met criteria for AAMI and 4 (15%) who did not meet criteria for either AAMI or mild cognitive impairment. The nondemented subjects had memory performance scores within the norms for cognitively intact persons of the same age and educational level (Table 1). The APOE-4 carriers had a small but consistent nonsignificant reduction in cognitive performance, and demented subjects showed the expected lower memory performance consistent with their diagnosis (Table 1).

As predicted, baseline comparisons among the three subject groups (ROI analysis) indicated the lowest metabolic rates for the AD group, intermediate rates for the nondemented APOE-4 carriers, and highest rates for the nondemented group without APOE-4 in several cortical regions (Fig. 1.). After Bonferroni correction, these differences were bilateral and significant (ANOVAs; df = 5,59) in inferior parietal (left hemisphere: $F = 9.2$, $P = 0.0036$; right hemisphere: $F = 14.6$, $P = 0.0012$), and posterior cingulate (left: $F = 25.0$, $P = 0.0012$; right: $F = 17.7$, $P < 0.0001$). Significant group differences present only in the left hemisphere were found in the dorsolateral prefrontal region ($F = 13.7$, $P = 0.0012$). Further ROI comparisons between the two nondemented groups included only these regions.

Baseline PET measures of the nondemented subjects (ROI analysis) indicated significantly lower metabolism in APOE-4 carriers in the inferior parietal region for both the right ($t = 2.4$, df = 50, $P = 0.019$) and left ($t = 2.3$, df = 50, $P = 0.026$) hemispheres compared with those without APOE-4. These differences remained significant even if we eliminated from the comparison the two subjects homozygous for APOE-4. Correcting for the small but consistent baseline reduction in cognitive performance in APOE-4 carriers had minimal effect on the results. The SPM analysis showed similar results: the APOE-4 carriers had significantly lower metabolism than those without APOE-4, particularly in the left inferior parietal, lateral temporal, and posterior cingulate regions (Fig. 2).

The 10 APOE-4 carriers available for longitudinal study were similar to the 10 noncarriers in mean ± SD age (67.9 ± 8.9 vs. 69.6 ± 8.1 years), educational achievement (14.4 ± 1.8 vs. 16.4 ± 2.8 years), and frequency of women (60 vs. 50%), dementia family history (60 vs. 40%), or AAMI (80 vs. 90%) or mild cognitive impairment (10 vs. 0%) diagnosis. Memory performance scores did not differ significantly according to genetic risk either at baseline or follow-up, and the APOE-4 carriers and noncarriers did not differ significantly in cognitive change after 2 years (Table 2). Baseline glucose metabolic rates in several ROIs, however, did predict memory performance decline in subjects with APOE-4 (Fig. 3).

The ROI analysis of PET scans performed after 2 years showed significant glucose metabolic decline (4%) in the left posterior cingulate region ($t = 2.8$, df = 9, $P = 0.022$) in APOE-4 carriers. The difference in decline between APOE-4 carriers and noncarriers, however, was not significant using the ROI data. The SPM analysis showed significant metabolic decline with the

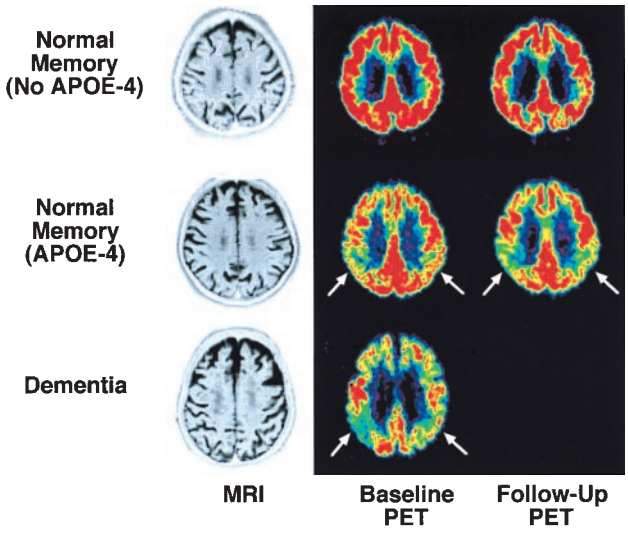

Fig. 1. Examples of PET images (comparable parietal lobe levels viewed from below head) coregistered to each subject's baseline MRI scan for an 81-year-old nondemented woman (APOE 3/3 genotype; *Top*), a 76-year-old nondemented woman (APOE 3/4 genotype; *Middle*), and 79-year-old woman with AD (APOE 3/4 genotype; *Bottom*). The last column shows 2-year follow-up scans for the nondemented women. Compared with the nondemented subject without APOE-4, the nondemented APOE-4 carrier had 18% (*Right*) and 12% (*Left*) lower inferior parietal cortical metabolism, whereas the demented woman's parietal cortical metabolism was 20% (*Right*) and 22% (*Left*) lower, as well as more widespread metabolic dysfunction due to disease progression. Two-year follow-up scans showed minimal parietal cortical decline for the woman without APOE-4, but bilateral parietal cortical decline for the nondemented woman with APOE-4, who also met clinical criteria for mild AD at follow-up. MRI scans were within normal limits.

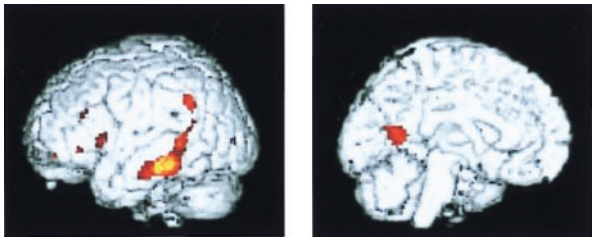

Fig. 2. Differences in cerebral metabolism in nondemented subjects according to genetic risk (SPM analysis). Lower metabolic levels are seen for the APOE-4 group (yellow and red areas) in left lateral temporal ($P < 0.001$), posterior cingulate ($P < 0.001$), and inferior parietal ($P < 0.006$) cortex. The region of peak significance ($z = 3.24$) lies in the temporal cortex in Brodmann's areas 20 and 21. Images are MRI structural images with superimposed SPM findings from PET.

Table 2. Baseline and 2-year follow-up cognitive performance scores on nondemented subjects in longitudinal study

	Subject groups	
	With APOE-4 (n = 10)	Without APOE-4 (n = 10)
Mini-mental state exam		
Baseline	28.0 ± 1.3	29.0 ± 1.3
Follow-up	28.0 ± 2.1	28.7 ± 1.3
Delayed paragraph recall		
Baseline	14.7 ± 6.6	18.4 ± 4.3
Follow-up	13.6 ± 7.5	20.2 ± 8.3
Buschke-Fuld total recall*		
Baseline	87.9 ± 14.0	95.2 ± 20.9
Follow-up	70.4 ± 29.4	94.2 ± 21.5
Benton visual errors		
Baseline	4.7 ± 2.6	6.1 ± 3.1
Follow-up	5.4 ± 3.7	3.8 ± 2.1

An ANCOVA model using follow-up scores as outcomes and baseline scores as covariates yielded no significant difference between groups in any of the measures. Values are reported as mean ± SD or number (percent).
*Baseline vs. follow-up for APOE-4 carriers: t = 2.5, df = 9, P = 0.036 (uncorrected).

greatest magnitude (5%) of metabolic decline in the inferior parietal and lateral temporal cortices (Fig. 4). After correction for multiple comparisons, this decline remained significant for the APOE-4 group (P = 0.02), wherein a decrease in metabolism was documented for every subject (Fig. 5). By contrast, the group without APOE-4 did not show significant metabolic decline at this location (z = 2.33, P = 0.998, corrected). Significant decline in that group was observed primarily in frontal cortex (P = 0.04), consistent with normal aging.

Discussion

These results extend previous investigations of nondemented APOE-4 heterozygotes at risk for familial AD (12) and APOE-4 homozygotes (22) and show that a single copy of the APOE-4 allele is associated with lowered inferior parietal, temporal, and posterior cingulate cortical metabolism in people with normal memory performance. Moreover, in subjects at genetic risk for AD, lower baseline metabolism predicted future cognitive decline, and the greatest metabolic decline after 2 years was observed in the parietal and temporal cortices, areas that show extensive early deposition of neuropathological lesions in patients with AD (5, 6).

These results have considerable practical implications. Comparison of the adjusted right lateral temporal metabolism for the APOE-4 group at baseline and 2-year follow-up indicated no overlap between data points in a relatively small sample of 10 subjects (Fig. 4). These data yield an estimated power under the most conservative scenario (i.e., assuming that the points are connected exactly in reverse order) of 0.9 to detect a 1-unit decline from baseline to follow-up by using a one-tailed test. A sample size of only 20 subjects would be needed in each treatment arm (i.e., active drug or placebo) to detect a drug effect size of 0.8 (α = 0.05, power = 0.8). Thus, a clinical trial of a novel intervention to prevent cerebral metabolic decline would require only 40 subjects over a 2-year treatment period. Such findings are consistent with previous PET studies showing stable and replicable results (37) and suggest that combining

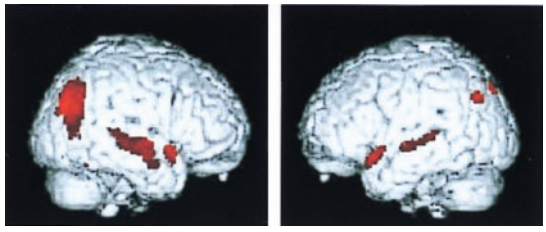

Fig. 4. Regions showing the greatest metabolic decline after 2 years of longitudinal follow-up in nondemented subjects with APOE-4 (SPM analysis) included the right lateral temporal and inferior parietal cortex (brain on the left side of figure). Voxels undergoing metabolic decline ($P < 0.001$, before correction) are displayed in color, with peak significance (z = 4.35) occurring in Brodmann's area 21 of the right middle temporal gyrus.

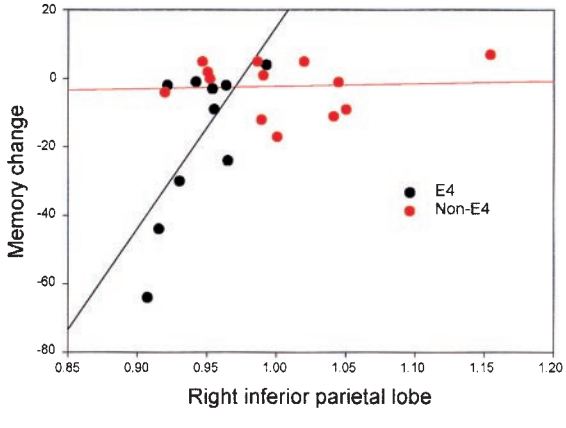

Fig. 3. The plot of the Buschke-Fuld recall change score (last to first) versus baseline right inferior parietal cortical metabolism indicated that lower baseline metabolism correlated with memory decline after 2 years in nondemented APOE-4 subjects (Pearson's r = 0.69, P = 0.026) but not in subjects without APOE-4. Other baseline regional metabolic rates correlating with memory change scores in APOE-4 subjects included left posterior cingulate cortex versus delayed paragraph recall (r = 0.67, P = 0.049) and right posterior cingulate cortex versus delayed paragraph recall (r = 0.71, P = 0.034). Baseline regional metabolic rates did not correlate with memory change scores in the nondemented subjects without APOE-4.

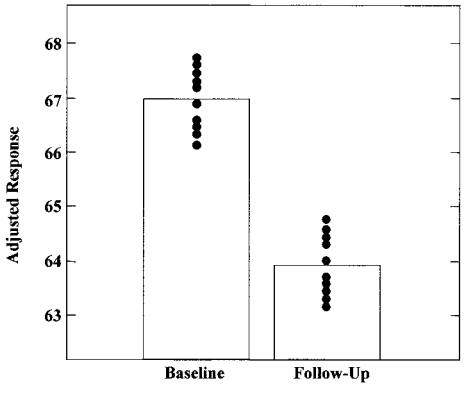

Fig. 5. Right lateral temporal metabolism (normalized to a mean voxel value of 50 for each brain and labeled adjusted response) for the APOE-4 subjects declined 5% at follow-up 2 years after baseline scans. Individual values (●) at the voxel of most significant decline (Talairach coordinates 68 −30 0) uniformly decreased, with no overlap for the two points in time (z = 4.35, P = 0.022, corrected for multiple comparisons). Although single voxels were initially defined for a volume of 8 mm^3, as the image data were preprocessed with a Gaussian-weighted three-dimensional smoothing filter of 16 mm FWHM (full width at half maximum) before statistical analysis, the data represent cerebral activity extending well beyond the confines of the brain tissue represented by the specific voxel location described by the given coordinates. Histograms represent means at each time point.

PET and AD genetic risk measures will allow investigators to use relatively small sample sizes when testing anti-dementia treatments in preclinical AD stages.

We also found frontal cortical metabolic decline in subjects without APOE-4, which is consistent with previous reports of normal age-related decline in anterior brain function (38). Such frontal decline probably was not observed in the APOE-4 carriers because the imaging data were normalized to whole brain gray matter and, in the APOE-4 carriers, the posterior portions of the cortex decreased more rapidly than the anterior ones. It is also not surprising that results varied somewhat according to analytic method. The ROI approach depends on *a priori* assumptions on size and shape of regions defined by structural criteria. If functionally relevant areas deviate from *a priori* assumptions, an area not functionally involved will dilute the statistical effect. By contrast, SPM analysis relies on pooled brain images spatially normalized into a common space, to the extent that the original sizes and shapes of brains differ will inevitably introduce some error.

We found that glucose metabolic rates correlated with memory performance decline 2 years later in APOE-4 carriers. Not all correlations were consistent with known hemispheric functions, but other AD functional imaging studies have shown that right-sided deficits correlate with verbal memory decreases and left-sided deficits predict verbal and visual memory decline (39). The APOE gene explains only about 50% of the genetic variability in AD, and efforts are ongoing to identify additional genetic risks (40). As other genetic risk factors are discovered, the utility of combined PET and genetic data in predicting cognitive decline would likely improve. Inspection of Fig. 3 indicates that of the subjects available for follow-up, those with APOE-4 had both greater baseline metabolic deficits and cognitive decline than those without APOE-4. As more of these subjects become available in longitudinal follow-up studies, we will augment our database on metabolic and cognitive decline rates, as well as conversion rates to an AD diagnosis.

The observation that metabolic patterns predict cognitive decline in presymptomatic persons indicates that the pathophysiologic process begins well before even mild or questionable dementia is recognized clinically. PET measures of hypometabolism reflect decreased synaptic activity due either to loss or dysfunction of synapses (41), and regional metabolic deficits observed on PET may reflect projections from dysfunctional neurons in other brain regions. Lesions of entorhinal cortex in non-human primates cause neocortical and hippocampal glucose hypometabolism (42), suggesting that the parietal and temporal cortical deficits observed in our study indicate underlying deficits in brain areas showing the earliest neuropathological changes in AD (5). Our finding of lowered cerebral metabolism in subjects with normal neuropsychological function also is consistent with studies (43) showing that the brain compensates for regional neuronal dysfunction leading to normal clinical neuropsychological performance, although biological degeneration is occurring.

In developing clinically useful data for predicting cognitive decline, measures of regional cerebral atrophy may provide additional information that could augment data on cerebral metabolic rates (44). Reduced PET measures of glucose metabolism in AD remain even after accounting for partial volume effects; thus, it is more than just an artifact resulting from increased cerebral spinal fluid space (45). Structural MRI measures of hippocampal atrophy appear to be less sensitive than functional measures by using PET in presymptomatic subjects at risk for AD (46). The present work represents an initial step in acquiring serial PET data from subjects at risk for AD. Such information will indicate the rate of change in metabolic activity for persons with different genotypes and allow the correlation of metabolic dysfunction of brain structures with the onset time of clinical symptoms.

Cholinesterase inhibitors have proven efficacy early in the disease course, which probably will be true of other treatments (4, 11). Moreover, if disease-modifying treatments are developed to slow the degenerative process, it will be critical to apply them early before extensive degeneration occurs. Early disease detection also will have economic consequences: preclinical patients could be treated earlier, resulting in better daily functioning and quality of life. Cholinesterase inhibitor treatments (47, 48) as well as nonpharmacological interventions (49) delay nursing home placement in patients with AD. The possibility that preclinical AD may be recognized early by using PET imaging and genetic risk assessment would facilitate early anti-dementia intervention and other possible functional gains in presymptomatic populations. Offsetting the costs of anti-dementia medications would be the savings from delaying lost productivity in the work force and avoiding repetitive and unnecessary examinations when diagnosis is uncertain.

In summary, we have demonstrated the consistency of cerebral metabolic deficits in middle-aged and older people with the APOE-4 genetic risk for AD and shown that baseline PET patterns predict future cognitive and metabolic decline after 2 years. Unlike other imaging techniques, PET can differentiate AD from benign effects of aging, as well as separate out other organic dementias, producing a pure AD population for testing therapies. In conjunction with APOE and other genotypic data, PET can assist in determining the time course for cerebral metabolic progression of the disease, provide homogeneous subject groups for study in experimental therapy protocols, and offer an objective and noninvasive approach to presymptomatic metabolic monitoring during experimental therapeutic trials.

We thank Ron Sumida and Larry Pang for their help in performing PET scans, Jennifer Bramen and Magdalena Strojwas for assistance in ROI determinations, and Dr. Donna Masterman, Andrea Kaplan, Deborah Dorsey, R.N., and Gwendolyn Byrd for their efforts in subject recruitment. This work was supported by Grants MH52453, AG13308, AG10123, RG2-96-051, NS31153, NS26630, AG05128, AG100784, AG16570, and AG11268 from the National Institutes of Health; MO1 RR00865 from the U.S. Public Health Service; IIRG94101 from the Alzheimer's Association; 95-23330 from the California Department of Health Services; the Department of Energy; the Sidell-Kagan Foundation; the Montgomery Street Foundation; the Fran and Ray Stark Foundation Fund for Alzheimer's Disease Research; the Parlow-Solomon Chair on Aging (UCLA School of Medicine); the Brain Mapping Medical Research Organization; the Ahmanson Foundation; and the Tamkin Foundation.

1. Ritchie, K. & Kildea, D. (1995) *Lancet* **346,** 931–934.
2. Evans, D. A. (1990) *Milbank Q.* **68,** 267–289.
3. Ernst, R. L. & Hay, J. W. (1994) *Am. J. Public Health* **84,** 1261–1264.
4. Small, G. W., Rabins, P. V., Barry, P. P., Buckholtz, N. S., DeKosky, S. T., Ferris, S. H., Finkel, S. I., Gwyther, L. P., Khachaturian, Z. S., Lebowitz, B. D., *et al*. (1997) *J. Am. Med. Assoc.* **278,** 1363–1371.
5. Braak, H. & Braak, E. (1991) *Acta Neuropathol.* **82,** 239–259.
6. Price, J. L. & Morris, J. C. (1999) *Ann. Neurol.* **45,** 358–368.
7. Arai, T., Ikeda, K., Akiyama, H., Haga, C., Usami, M., Sahara, N., Iritani, S. & Mori, H. (1999) *Acta Neuropathol.* **97,** 82–84.
8. Beach, T. G., Honer, W. G. & Hughes, L. H. (1997) *Acta Neuropathol.* **93,** 146–153.
9. Petersen, R. C., Smith, G. E., Waring, S. C., Ivnik, R. J., Tangalos, E. G. & Kokmen, E. (1999) *Arch. Neurol.* **56,** 303–308.
10. Crook, T., Bartus, R. T., Ferris, S. H., Whitehouse, P., Cohen, G. D. & Gershon, S (1986) *Dev. Neuropsychol.* **2,** 261–276.
11. Rogers, S. L. & Friedhoff, L. T. (1996) *Dementia* **7,** 293–303.
12. Small, G. W., Mazziotta, J. C., Collins, M. T., Baxter, L. R., Phelps, M. E., Mandelkern, M. A., Kaplan, A., La Rue, A., Adamson, C. F., Chang, L., *et al*. (1995) *J. Am. Med. Assoc.* **273,** 942–947.

13. Saunders, A. M., Strittmatter, W. J., Schmechel, D., George-Hyslop, P. H. S., Pericak-Vance, M. A., Joo, S. H., Rosi, B. L., Gusella, J. F., Crapper-MacLachlan, D. R., Alberts, M. J., *et al*. (1993) *Neurology* **43,** 1467–1472.
14. Corder, E. H., Saunders, A. M., Strittmatter, W. J., Schmechel, D. E., Gaskell, P. C., Small, G. W., Roses, A. D., Haines, J. L. & Pericak-Vance, M. A. (1993) *Science* **261,** 921–923.
15. Corder, E. H., Saunders, A. M., Risch, M. J., Strittmatter, K. E., Schmechel, W. J., Gaskell, D. E., Small, G. W., Roses, A. D., Haines, J. L., Rimmler, J. B., *et al*. (1994) *Nat. Genet.* **7,** 180–183.
16. Hyman, B. T., Gomez-Isla, T., Briggs, M., Chung, H., Nichols, S., Kohout, F. & Wallace, R. (1996) *Ann. Neurol.* **40,** 55–66.
17. Phelps, M. E., Mazziotta, J. C. & Huang, S. C. (1982) *J. Cereb. Blood Flow Metab.* **2,** 113–162.
18. Phelps, M. E. & Mazziotta, J. C. (1985) *Science* **228,** 799–809.
19. Phelps, M. E., Huang, S. C., Hoffman, E. J., Selin, C., Sokoloff, L. & Kuhl, D. E. (1979) *Ann. Neurol.* **6,** 371–388.
20. Huang, S. C., Phelps, M. E., Hoffman, E. J., Sideris, K., Selin, C. J. & Kuhl, D. E. (1980) *Am. J. Physiol.* **238,** E69–82.
21. Silverman, D. H. S., Small, G. W. & Phelps, M. E. (1999) *Clin. Positron Imaging* **2,** 119–130.
22. Reiman, E. M., Caselli, R. J., Yun, L. S., Chen, K., Bandy, D., Minoshima, S., Thibodeau, S. N. & Osborne, D. (1996) *N. Engl. J. Med.* **334,** 752–758.
23. Crum, R. M., Anthony, J. C., Bassett, S. S. & Folstein, M. F. (1993) *J. Am. Med. Assoc.* **269,** 2386–2391.
24. Wechsler, D. A. (1981) *Wechsler Memory Scale-Revised* (Psychological Corp., New York).
25. Buschke, H. & Fuld, P. A. (1974) *Neurology* **24,** 1019–1025.
26. Benton, A. L. (1974) *The Revised Visual Retention Test* (Psychological Corp., New York).
27. McKhann, G., Drachman, D., Folstein, M., Katzman, R., Price, D. & Stadlan, E. M. (1984) *Neurology* **34,** 939–944.
28. Corder, E. H., Jelic, V., Basun, H., Lannfelt, L., Valind, S., Winblad, B. & Nordberg, A. (1997) *Arch. Neurol.* **54,** 273–277.
29. Hirono, N., Mori, E., Yasuda, M., Ishii, K., Ikejiri, Y., Imamura, T., Shimomura, T., Hashimoto, M., Yamashita, H. & Sasaki, M. (1998) *Alzheimer Dis. Assoc. Disord.* **12,** 362–367.
30. Lin, K. P., Huang, S. C., Baxter, L. & Phelps, M. E. (1994) *IEEE Trans. Nucl. Sci.* **41,** 2850–2855.
31. Talairach, J. & Tournoux, P. (1988) *Coplanar Stereotaxic Atlas of the Human Brain. Three-Dimensional Proportional System: An Approach to Cerebral Imaging* (Thieme, New York).
32. Rottenberg, D. A., Moeller, J. R., Strother, S. C., Dhawan, V. & Sergi, M. L. (1991) *J. Cereb. Blood Flow Metab.* **11,** A83–A88.
33. Friston, K. J., Ashburner, J., Frith, C. D., Poline, J., Heather, J. D. & Frackowiak, R. S. J. (1995) *Hum. Brain Mapping* **2,** 165–189.
34. Friston, K. J., Holmes, A., Poline, J. B., Price, C. J. & Frith, C. D. (1996) *NeuroImage* **4,** 223–235.
35. Silverman, D. H., Munakata, J. A., Ennes, H., Mandelkern, M. A., Hoh, C. K. & Mayer, E. A. (1997) *Gastroenterology* **112,** 64–72.
36. Friston, K. J., Holmes, A. P., Worsley K. J., Poline, J. P., Frith, C. D. & Frackowiak, R. S. J. (1995) *Hum. Brain Mapping* **2,** 189–210.
37. Andreasen, N. C., Arndt, S., Cizadlo, T., O'Leary, D. S., Watkins, G. L., Ponto, L. L. & Hichwa, R. D. (1996) *J. Cereb. Blood Flow Metab.* **16,** 804–816.
38. Mielke, R., Kessler, J., Szelies, B., Herholz, K., Wienhard, K. & Heiss, W. D. (1998) *J. Neural Transm.* **105,** 821–837.
39. Keilp, J. G., Alexander, G. E., Stern, Y. & Prohovnik, I. (1996) *Brain Cognit.* **32,** 365–383.
40. Pericak-Vance, M. A., Bass, M. P., Yamaoka, L. H., Gaskell, P. C., Scott, W. K., Terwedow, H. A., Menold, M. M., Conneally, P. M., Small, G. W., Vance, *et al*. (1997) *J. Am. Med. Assoc.* **278,** 1237–1241.
41. Mazziotta, J. C. & Phelps, M. E. (1986) in *Positron Emission Tomography and Autoradiography: Principles and Applications for the Brain and Heart*, eds. Phelps, M., Mazziotta, J. & Schelbert, H. (Raven, New York), pp. 493–579.
42. Meguro, K., Blaizot, X., Kondoh, Y., Le Mestric, C., Baron, J. C. & Chavoix, C. (1999) *Brain* **122,** 1519–1531.
43. Grady, C. L., Haxby, J. V., Horwitz, B., Gillette, J., Salerno, J. A., Gonzalez-Aviles, A., Carson, R. E., Herscovitch, P., Schapiro, M. B. & Rapoport, S. I. (1993) *Neurobiol. Aging* **14,** 35–44.
44. Jack, C. R., Peterson, R. C., Xu, Y. C., Waring, S. C., O'Brien, P. C., Tangalos, E. G., Smith, G. E., Ivnik, R. J. & Kokmen, E. (1997) *Neurology* **49,** 786–794.
45. Ibáñez, V., Pietrini, P., Alexander, G. E., Furey, M. L., Teichberg, D., Rajapakse, J. C., Rapoport, S. I., Schapiro, M. B. & Horwitz, B. (1998) *Neurology* **50,** 1585–1593.
46. Reiman, E. M., Uecker, A., Caselli, R. J., Lewis, S., Bandy, D., de Leon, M. J., De Santi, S., Convit, A., Osborne, D., Weaver, A. & Thibodeau, S. N. (1998) *Ann. Neurol.* **44,** 288–291.
47. Knopman, D., Schneider, L. S., Davis, K. Talwalker, S., Smith, F., Hoover, T., Gracon, S. & the Tacrine Study Group. (1996) *Neurology* **47,** 166–177.
48. Small, G. W., Donohue, J. A. & Brooks, R. L. (1998) *Clin. Ther.* **20,** 838–850.
49. Mittelman, M. S., Ferris, S. H., Shulman, E., Steinberg, G. & Levin, B. (1996) *J. Am. Med. Assoc.* **276,** 1725–1731.